# Electronic properties of nascent GaP(110)–noble-metal interfaces

R. Ludeke, A. B. McLean,* and A. Taleb-Ibrahimi†
*IBM Research Division, Thomas J. Watson Research Center, P.O. Box 218, Yorktown Heights, New York 10598*
(Received 11 January 1990; revised manuscript received 18 April 1990)

The evolution of the interface properties of cleaved *n*-type and *p*-type GaP(110) surfaces with Ag, Cu, and Au overlayers was investigated by photoemission spectroscopy excited with synchrotron radiation. Silver was found to be relatively unreactive with GaP, although some evidence for a Ga replacement reaction was found. Cu and especially Au were observed to react strongly with GaP, with clear evidence of metal-Ga exchange reactions occurring for coverages of $\gtrsim 0.3$ Å. Phosphorus-metal reaction products include Cu-P and Au-P components characterized by a P $2p$ binding energy comparable to that of P in GaP. An additional reaction product was observed for Au, which was tentatively interpreted as elemental P. All phosphorus components tend to diffuse to the metal surface. The band bending, or specifically the position of the interface Fermi level $E_F$ relative to the band edges, was measured as a function of metal coverage. On *n*-type surfaces $E_F$ remained fairly constant for coverages to $\sim 1$ Å, but dropped lower into the band gap as the overlayer assumed metallic properties. On *p*-type surfaces $E_F$ increased for low coverages, but decreased at the onset of metallicity (overshoot). For coverages $\gtrsim 10$ Å, $E_F$ reached a common value on *n*- and *p*-type surfaces, which differed among the metals. Measured Schottky-barrier heights $\Phi_B^n$ for *n*-type GaP(110) were 1.55 eV (Au), 1.37 eV (Ag), and 1.41 eV (Cu). The delocalization model was applied to calculate both the drop in $E_F$ with metallization, and $\Phi_B^n$ for the three metals. Agreement with experiments supports the model and underscores the importance of defect and metallic states in Schottky-barrier physics.

## I. INTRODUCTION

Much of our present understanding of the metal-semiconductor interface derives from the extensive work on Si and GaAs,[1] which served as prototypes for the development of various models addressing the origin of the Schottky barrier. Less attention has been given to other compound semiconductor-metal interfaces and particularly little is known about their behavior for low metal coverages, at which the electronic properties of the interface develop. These properties, e.g., the Schottky-barrier heights, appear to be fully developed at metal coverages of less than $\sim 5$ monolayers (ML) of the metal for GaAs and InP.[2–4] Recently, it was observed that for a few metals on GaAs the barrier heights were fully established only after the overlayer developed its metallic characteristics.[5–7] In retrospect a similar conclusion can be arrived at from earlier data.[4,8–10] These observations were interpreted in terms of favoring specific models, such as the metal-induced gap-state (MIGS) models,[11–15] or the recently proposed delocalization model.[16,17] It is thus of general interest to investigate other metal-semiconductor systems in order to assess the generality of interface behavior already observed on GaAs and InP, as well as to test the applicability of existing models to the new systems.

Some of the key aspects previously observed for GaAs include: (i) a metal dependence of Schottky-barrier heights exceeding 0.25 eV,[1,17–19] (ii) a common interface Fermi-level position ($E_F$) for *n*- and *p*-type samples for thick metallic coverages, and (iii) barrier-height readjustments with onset of metallic characteristics in the overlayer. The latter always results in a decrease of $E_F$ relative to the GaAs valence-band maximum (VBM), or equivalently an increase of the band bending (barrier height) with metal coverage for *n*-type samples, and a decrease for *p*-type samples. On *p*-type GaAs(110), $E_F$ may increase relative to the VBM with coverage before reversing this trend with onset of overlayer metallicity. This "overshoot," although observed for room-temperature depositions,[4,20] is particularly pronounced for low-temperature depositions,[9,10] and represents a dramatic manifestation of the transition from metal-adatom-induced adsorbate,[21] defect levels,[2,22] or impurity states[8,17] for submonolayer coverages, to metal-induced[11–15] or metal-modified[17] interface states for thick metallic coverages.

Prior transport measurements of Schottky-barrier heights on *n*-type GaP indicated metal-work-function-dependent variations of $\sim 0.3$–$0.4$ eV,[23,24] which exceed those for GaAs ($\sim 0.25$ eV). This range is still only about $\frac{1}{4}$ of the spread in work-function values used in the experiments, and represents a large deviation from the ideal Schottky-Mott behavior.[1] However, a prior photoemission study on *n*-type GaP(110) claimed nearly ideal Schottky behavior.[25] This large discrepancy between transport and photoemission measurements appears unusual, as it is not observed for GaAs.[17] Clearly, this issue needs to be resolved, preferably through a detailed low-coverage photoemission study, which at the same time tests the generality of issues discussed above for GaAs. This approach is taken here, although we limit

 

ourselves in this study to the noble metals Cu, Ag, and Au on both $n$ and $p$-type GaP substrates. The choice of different doping types has the added advantage of a consistency check for the band-bending data, as a precise determination of $E_F$ may be difficult to assess from a single data set. This problem is enhanced because metals are generally more reactive on GaP than on GaAs, and this causes drastic line-shape changes in the core-level photoemission spectra from which the band bending is determined.[26]

Our principal conclusions of this study are the following: (i) variations in Schottky-barrier heights for the noble metals are small and do not follow the Schottky-Mott rule; (ii) $n$- and $p$-type samples exhibit the same final position of $E_F$ for coverages $\gtrsim 10$ Å of a given metal; (iii) on $n$-type GaP, $E_F$ exhibits a nearly constant value over a broad range of submonolayer coverages, followed by a decrease, $\Delta E_F$, with onset of metallic behavior near 1 ML (an overshoot behavior is observed on $p$-type GaP for the three metals); (iv) values of $\Delta E_F$ calculated within the framework of the delocalization model agree well with experiment; (v) Cu and Au react strongly with GaP, producing elemental Ga and up to two (for Au) phosphorus reaction products that diffuse to the surface; (vi) Ag is relatively unreactive on GaP, although a weak Ag-Ga exchange reaction is suggested by the data.

## II. EXPERIMENTAL DETAILS

The experiments were performed with the IBM beamline U8 on the vuv ring of the National Synchrotron Light Source (NSLS) at the Brookhaven National Laboratory (Upton, NY). The beamline consists of a combination of 6-m/10-m toroidal-grating monochromator and a display electron spectrometer; their combined resolution was $\sim 0.2$ and 0.3 eV for working photon energies of $h\nu = 80$ and 150 eV, respectively. The spectrometer was used in an angle-integrated mode, with an acceptance angle of 1.8 sr. A single grating was used for both photon energies. A separate sample-preparation chamber, with vacuum interlock to the analysis chamber, was used for cleaving and metal deposition. Zn-doped ($6\times10^{17}$ cm$^{-3}$) $p$-type and Te-doped ($2\times10^{17}$ cm$^{-3}$) $n$-type GaP(111) wafers were cut into rectangular bars of $4\times4$ mm$^2$ cross section, which were oriented lengthwise along a $\langle 110 \rangle$ direction. The bars were notched to facilitate the alignment of the cleaving blade. For the indicated doping concentrations the bulk Fermi levels for $n$- and $p$-type GaP are in the band gap at an energy of 100 meV from the band edges. The metal was deposited from a resistively heated, boron-nitride cell assembly that could be moved into the main preparation chamber through an interlock, an arrangement that allowed quick and convenient evaporant changes without breaking vacuum. Pressures during deposition were in the mid-$10^{10}$-Torr range. Metal evaporation rates were determined with a quartz thickness monitor from extended and repeated calibration runs, following long out-gassing and thermal stabilization periods. Reliable rates of as low as 1000 s/Å were readily obtained with relative repeat accuracies of $\pm 20\%$. Absolute thickness values were estimated to be of comparable uncertainty for coverages near and above 1 Å, with somewhat higher uncertainties for the lower coverages. Following either a good cleave or metal deposition, the sample was transferred to the analysis chamber for measurement of electron-distribution curves (EDC's) of the Ga $3d$ and P $2p$ core levels at $h\nu = 80$ and 150 eV, respectively, the valence band at 80 eV, and a broad-range survey spectrum at 150 eV, from which the attenuation of the core levels were evaluated. The Au-$4f$ level was measured as well for Au coverages exceeding 0.01 Å. In order to check consistency, two deposition sequences were generally made on each type of substrate, for a total of up to four runs per metal.

The spectra were digitally stored and transferred electronically to an IBM mainframe at the Thomas J. Watson Research Center. The core-level EDC's were analyzed by first subtracting a background curve that is proportional to the integral under the emission peak and which matches the background slope outside the peak. Then an interactive computer program synthesized a spectrum recursively from a pre-determined number of components until the least-squares deviation between the generated and the experimental spectra was less than 0.005, subject, of course, to the usual constraints of spin-orbit splittings, branching ratios and Lorentzian widths. The basic line shape was assumed to be a Lorentzian convoluted with a Guassian broadening function. Most fits required at least two spin-orbit-split components, which for low metal coverages consisted of the bulk and the surface components of the GaP substrate,[27] and for the highest coverages consisted of the bulk component plus one or two new components attributed to reaction products between substrate and metal. At intermediate coverages between $\sim 0.3$ and 5 Å three components were generally required. The reaction components in both P $2p$ and Ga $3d$ EDC's dominate the spectra for Au and Cu coverages exceeding 5 Å and restricted the accurate determination of the kinetic energy (KE) of the bulk component, which is used to determine the band bending. A somewhat more complicated analysis is required for the reacted Ga component in the Ga $3d$ spectra. Because the reacted Ga exhibits metallic character, its line shape is subject to an additional broadening on its low-KE side. The broadening is attributed to multi-particle excitations at the metallic Fermi edge; its effect on the line shape can be adequately described by a Doniach-Šunjić distribution.[28] The appropriate spectral line shape is a convolution of this distribution with the Lorentzian-Gaussian distribution.[4] Kinetic-energy shifts for the bulk component of the core-level spectra were measured with an accuracy of $\pm 20$ meV for Ag at all coverages and for Au and Cu for coverages up to 1 ML; for the latter two metals the accuracy deteriorated considerably to $\pm 50$ meV at coverages exceeding 3 ML. A ML is referred to the atomic density of $9.52\times10^4$ cm$^2$ of GaP(110). The thickness equivalence is 1.1 Å/ML for Cu and 1.61 Å/ML for Ag and Au.

## III. SPECTRAL ANALYSIS

### A. Ag/GaP

We begin our discussion with Ag, since its low reactivity with the GaP substrate makes the data analysis

straightforward. The spectral decompositions of the Ga 3*d* core level for representative coverages of 0, 0.01, 0.1, 1, and 10 Å of Ag on *n*-type GaP(110) are shown in Fig. 1. The line shape over most of the coverage range is similar to that of the clean surface, Fig. 1(a). It is characterized by a cleft main peak and a weak shoulder on the low-KE side. This structure, which is very similar to the Ga 3*d* spectrum of a well-cleaved GaAs(110) surface,[4] is indicative of a homogeneous surface potential, i.e., band bending is either negligibly small or distributed evenly (within dimensions of the Debye length) over the surface.

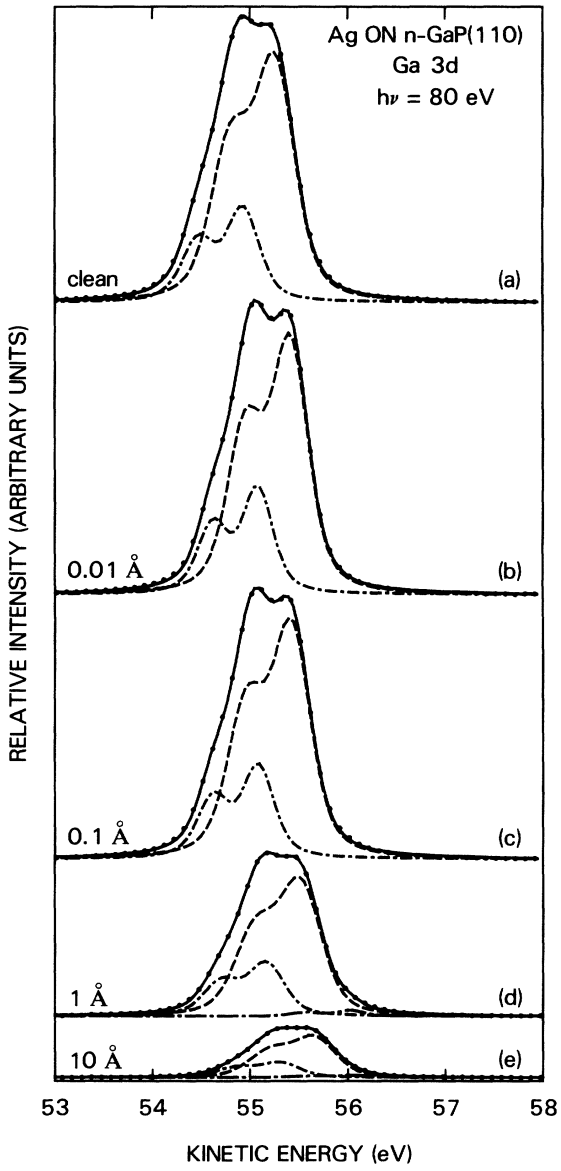


FIG. 1. Ga 3*d* spectra of Ag on *n*-type GaP(110) for indicated Ag coverages. The dots represent the experimental data. Each spectrum is decomposed into a bulk (dashed line) and a surface component (dashed-dotted line). For 1 and 10 Å coverages [curves (d) and (e)] a weak third component on the high-KE side of the bulk component was needed in the fits. The solid line through the experimental data represents the sum of all the components.

In comparison, the corresponding spectra for freshly cleaved *p*-type samples were always less resolved. However, small coverages of metal atoms will enhance spectral details (not shown) as the band bending became more homogeneous across the surface. We will readdress this point in the discussion section, as it bears directly on the issue of the position of the Fermi level for the well-cleaved *n*-type-GaP surface.[29,30] The spectra was decomposed into bulk and surface contributions, as indicated in Fig. 1 by dashed and dotted-dashed curves, respectively. The best-fit values of our fitting parameters, which are unconstrained variables in our routine, were essentially identical to our previously published values,[27] although an entirely different algorithm was used in the present case. The persistence of the surface component up to the maximum coverage of 100 Å (not shown) indicates, as for GaAs (Ref. 20) and previous work on GaP,[26] that the Ag growth consists of three-dimensional clusters which do not fully cover the GaP surface. The shifts of the emission structure toward higher KE in these spectra for *n*-type-GaP result from increases in band bending with Ag coverage. For Ag coverages in the 1–10-Å range, for which we still had good counting statistics, it became necessary to fit a weak ($\sim 2\%$ of the total line intensity) third peak on the high-KE side of the bulk structure. The discerning eye can observe the third contribution in curves (d) and (e) of Fig. 1. This component, which lies at a relative KE of $\sim 0.5$ eV above the bulk component, is consistent with elemental Ga, but not metallic Ga [a change in KE of $\sim 0.7$ eV (Ref. 31)]. Its presence in the four separate runs is statistically significant, and if not spurious, suggests that Ag interacts weakly with GaP.

The P 2*p* spectra for the same Ag coverages are shown in Fig. 2. They are again decomposed into bulk (dashed) and surface contributions (dotted-dashed), which again persist up to the maximum Ag coverage of 100 Å. As for the clean Ga 3*d* spectrum, the fitting parameters for the two components are practically identical to those previously published.[27] There is no evidence in these spectra of reaction products involving Ag and P. Our estimated sensitivity is 2–3 % for a component removed $\gtrsim 0.5$ eV from a major spectral component.

The attenuation curves of the Ga 3*d* and P 2*p* emission intensities, normalized to unity for the clean surface, are shown in Fig. 3. Their nonlinear and slow attenuations with coverage in this logarithmic plot are again indicative of three-dimensional cluster growth. The attenuation curve for the P 2*p* emission lies consistently below that for Ga 3*d*. We attribute this observation to a slightly greater surface sensitivity in the P 2*p* spectra (KE of $\sim 45$ eV), relative to the Ga 3*d* spectra (KE of $\sim 55$ eV).[27] The relatively large signal strengths at 100 Å of Ag indicates the presence of bare surface patches (pinholes), a conclusion which is consistent with the presence of the surface components in the Ga 3*d* and P 2*p* core-level spectra for the same coverage (not shown).

Additional details of the formation of the interface can be obtained from the valence-band spectra at various metal coverages. Representative spectra, including that of the clean surface for *n*-type GaP(110) are shown in Fig. 4. Superimposed on the clean spectrum [solid line,

curve (a)] is a spectrum, indicated by the dotted curve, for a Ag coverage of only 0.003 Å (0.002 ML). Their difference, after correcting for a band-bending change, is shown in curve (b), and represents extra emission arising from Ag 4*d* electrons. The great sensitivity is the consequence of both the large photoionization cross section of the 4*d* electrons at the chosen photon energies, which is ~100 times that of the *s* and *p* valence electrons of Ga and P,[32] and the favorable binding energy of the Ag 4*d* which overlaps the heterpolar gap of the GaP. The Ag 4*d* emission rapidly increases both in intensity and width and dominates the spectra at larger coverages. Its line shape evolves as well, from an essentially featureless and broadened singlet at the lowest coverage, to the doublet structure characteristic of metallic Ag, curve (f), which remains unchanged for higher Ag coverages. The line shape at 1 Å of Ag, and to some extent that at 0.5 Å [curves (d) and (e)], already exhibit the features of metallic Ag, although the width is narrower than the fully developed peak at 10 Å. The width of the Ag 4*d* emission has been used as a criterion to determine the onset of metallicity for Ag/GaAs.[33] A more convincing manifestation of this onset is the appearance of a metallic Fermi edge in the valence-band EDC's. We show in Fig. 5 expanded spectra for emission near the valence-band edge. Although emission electrons, presumably from the Ag 5*s* states,[20] already "tail" towards the energetic position of the future Fermi edge for 0.5 Å of Ag, the edge does not become evident until Ag coverages of ~1 Å. For Ag/GaAs the Fermi edge appeared at coverages nearly four times smaller,[20] which suggests a larger surface mobility (less interaction) for Ag on GaAs(110) than on GaP(110). The appearance of a Fermi edge is crucial in the development of the band bending that ultimately determines the Schottky barrier. This topic will be extensively discussed in Sec. IV, after we present and discuss the core-level analysis for Cu and Au on GaP.

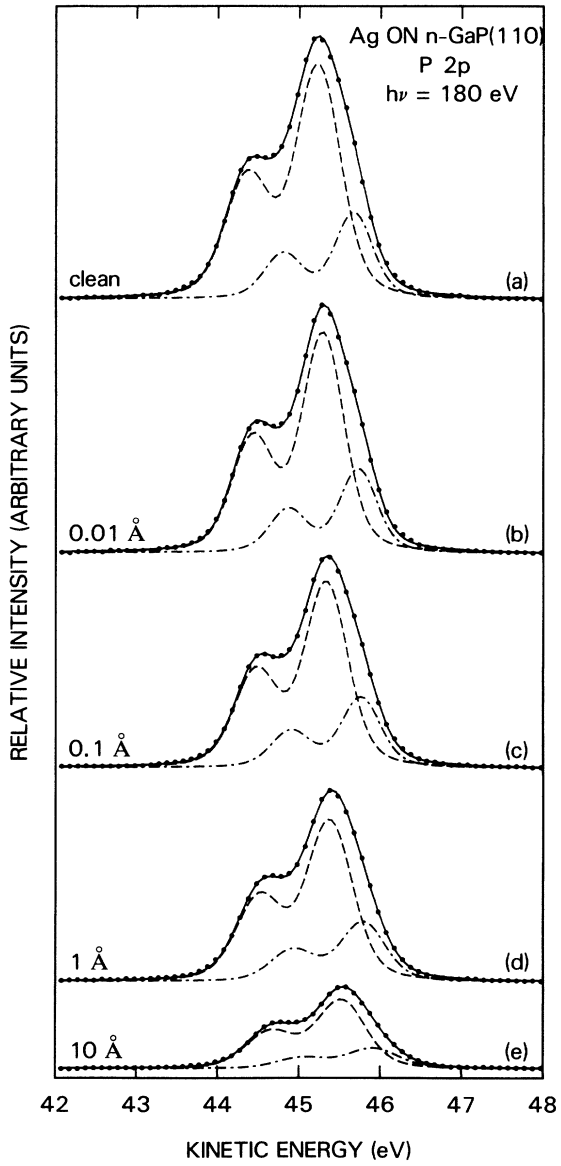


FIG. 2. P 2*p* spectra for Ag on *n*-type GaAs(110). The coverages and component designations are identical to those of Fig. 1.

### B. Cu/GaP(110)

The Ga 3*d* core-level spectra for the freshly cleaved *n*-type GaP(110) surface and for Cu coverages of 0.01, 0.1, 1, 5, and 10 Å are shown in Fig. 6. For this particular cleave it was necessary to initially include a third component on the high-KE side of the clean spectrum, Fig.

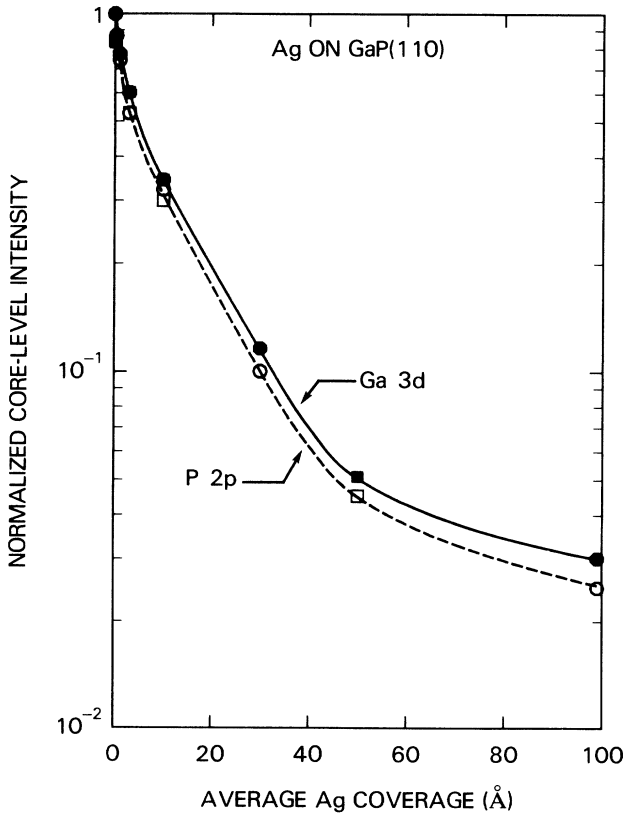


FIG. 3. Attenuation of the emission intensities of the Ga 3*d* and P 2*p* core levels with nominal Ag coverage.

6(a), which represents a small portion of the surface that was subjected to some cleavage-induced band bending of unknown origin. The addition of some Cu [curves (b) and (c)] causes the band bending to become homogeneous across the surface, as can be judged from a line shape comparison with the corresponding spectrum for Ag in Fig. 1. Generally we find that for surfaces which exhibit areas of different band bending the addition of $\lesssim 0.01$ ML of metal tends to increase the average band bending and equalize $E_F$ throughout the surface. This observation implies that any initial cleavage-induced band bending is caused by a relatively low density of defect states. These states are readily suppressed by the larger number of states produced during deposition, whose density is comparable to the number of deposited atoms.[21] We find that the band bending with coverage is reproducible and is independent of the initial position of $E_F$ for the cleaved surface. In contrast to Ag, Cu is the more reactive, as is evident in the Ga $3d$ core-level spectrum for 1 Å [Fig. 6(d)], which clearly indicates the presence of a shoulder on the high-KE side of the main peak. This structure already becomes evident in the spectral decompositions at 0.3 Å, and is consistent with the presence of elemental Ga liberated by an exchange reaction with the Cu. Its intensity increases with coverage and attains a value comparable to the intensity of the bulk component for a 10-Å coverage. Although not clearly evident from Fig. 6, the line shape of the replaced Ga component includes a Doniach-Šunjić contribution with an asymmetry factor of

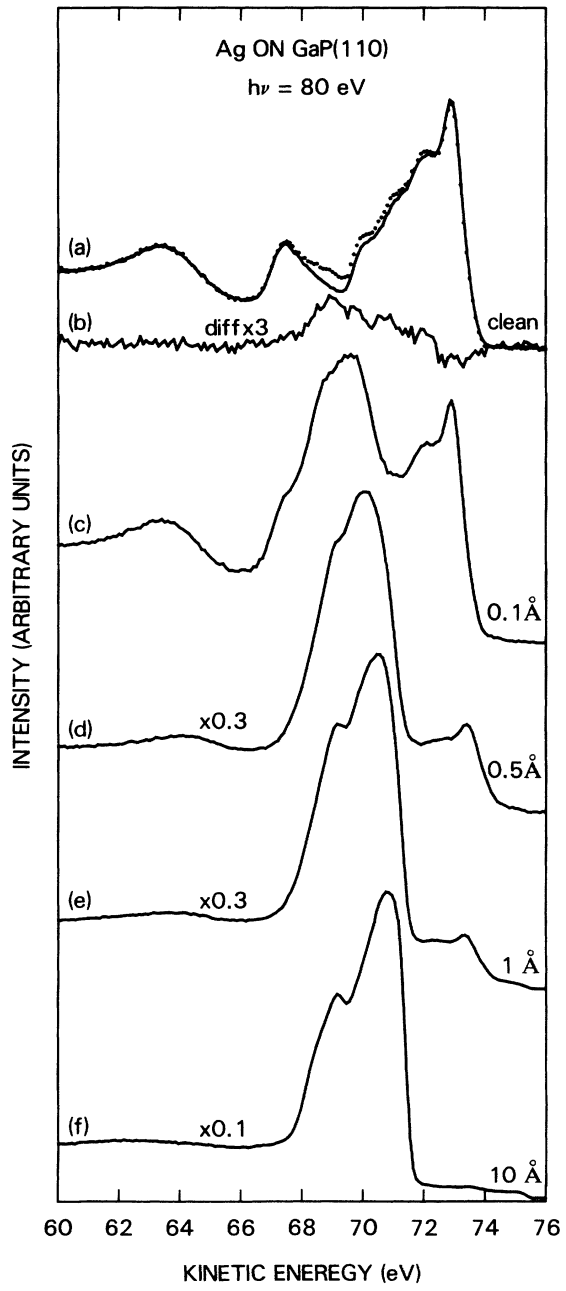


FIG. 4. Valence-band EDC's for clean $n$-type GaP(110), solid curve (a), and covered with 0.003 Å of Ag—dotted symbols in (a). Their difference is shown in curve (b). The remaining spectra (c) and (d) are for Ag coverages of 0.1, 0.5, 1, and 10 Å.

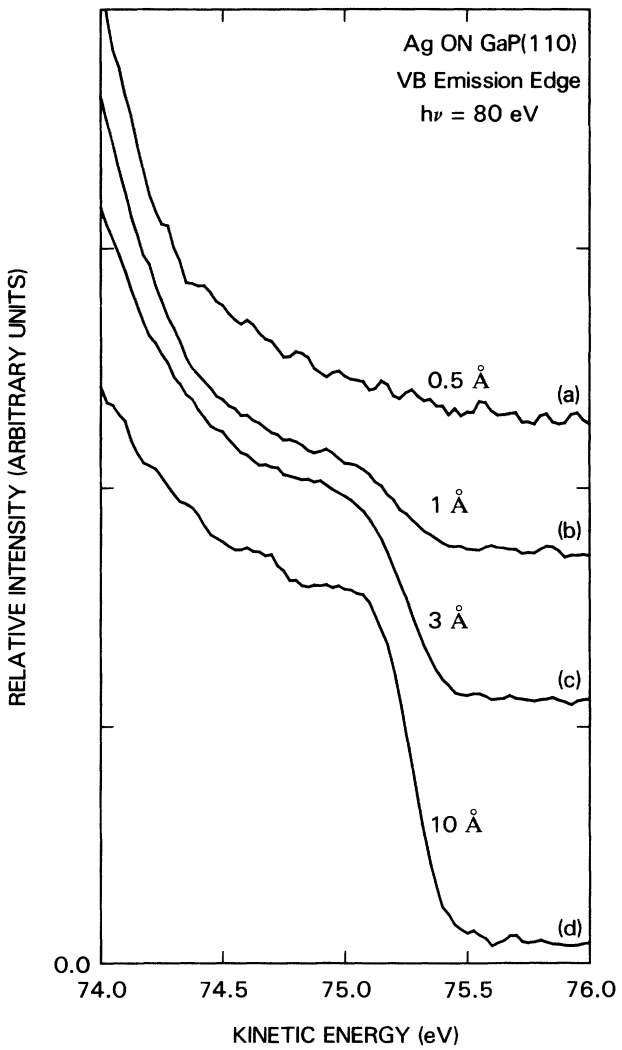


FIG. 5. Expanded view of the emission-edge region of the valence-band EDC's for Ag on GaP(110). The appearance of the metallic Fermi edge is evidence for 1 Å coverage, curve (b).

0.1, which clearly demonstrates that the replaced Ga is metallic. Moreover, the KE of this component relative to the bulk component is equal to the value of 0.7 eV found for Ga on GaAs(110),[31] which suggests that the Ga is aggregated and not extensively alloyed with Cu. It was also necessary to include the surface component into our fits for 5 Å (~4 ML) of Cu, which indicates that the Cu forms three-dimensional clusters as well. The Cu-Ga phase diagram[34] indicates a broad solid-solution region near room temperature, void of any compound phases.

The P 2*p* spectra for the corresponding Cu coverages are shown in Fig. 7. The clean-surface spectrum [curve (a)] is composed of just the bulk and surface components; the latter includes a shifted contribution from the bulk, as discussed for the Ga 3*d* spectrum of Fig. 6(a), which overlaps the surface peak and whose size cannot be independently determined. As a function of coverage, the surface contribution decreases and disappears beyond 5 Å, in agreement with the Ga 3*d* core-level data. A unique feature of these spectra is the apparent absence of a component attributable to Cu-P reactions, as the bulk component appears to remain the sole contributor to the P 2*p* spectra [e.g., curve (f)]. However, the P 2*p* attenuation curve, shown together with the Ga 3*d* and Cu 3*d* intensity curves in Fig. 8, reveals a tendency for the P 2*p*

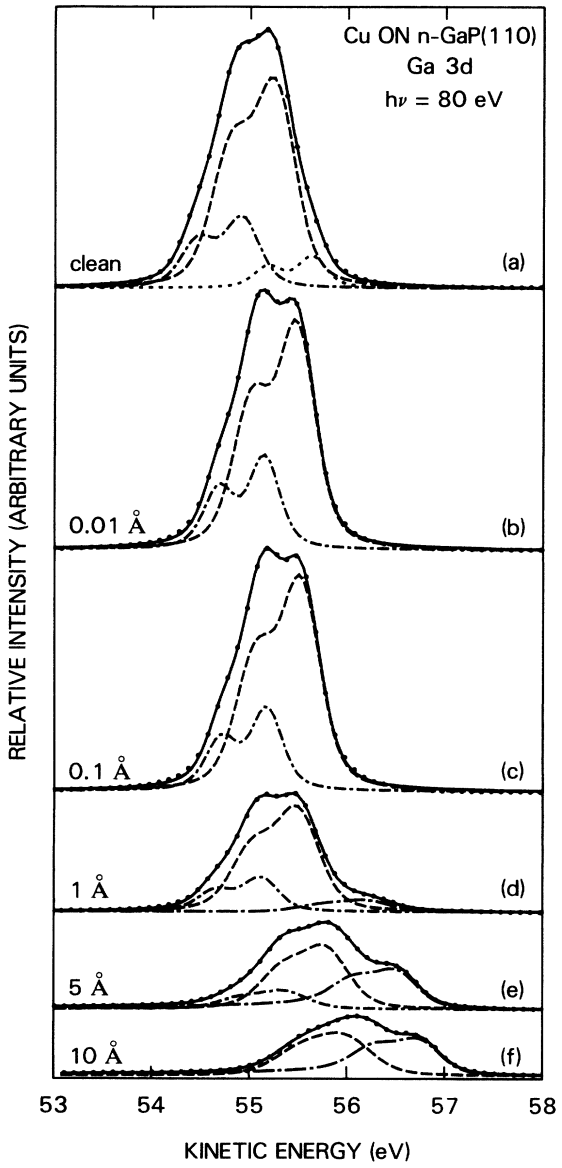


FIG. 6. Ga 3*d* spectra for indicated Cu coverages on *n*-type GaP(110). The line designations are the same as Fig. 1. The dotted component on the high-KE side of the clean surface spectrum is attributed to residual band bending, which vanishes with Cu coverage (see text). The long dotted-dashed component, seen in curves (d)–(f) on the high-KE side, is due to free Ga.

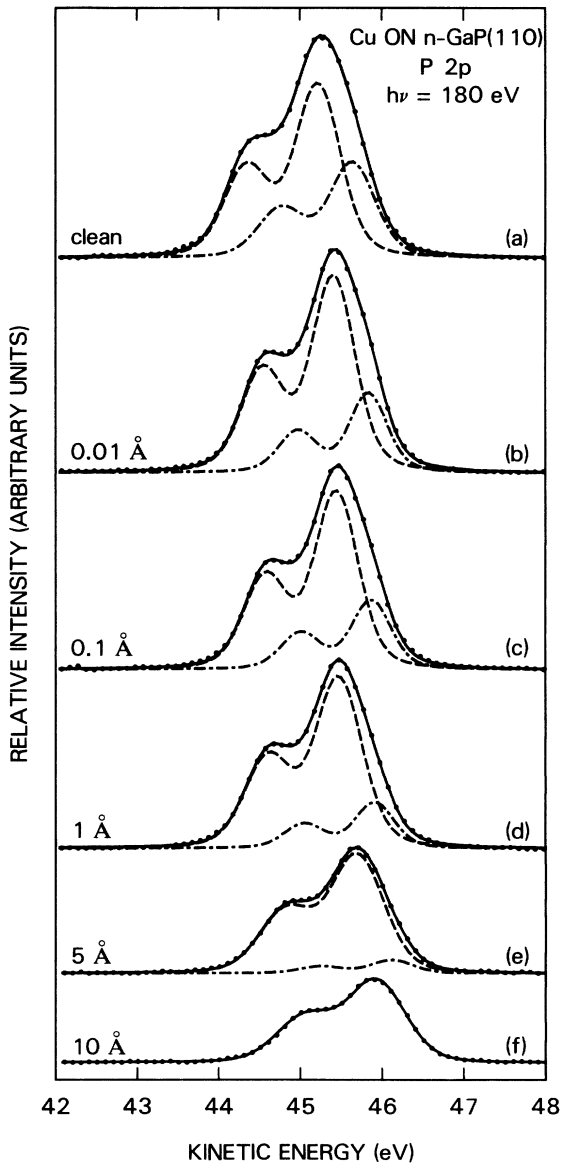


FIG. 7. P 2*p* spectra for indicated Cu coverages on *n*-type GaP(110). The surface component is detectable to coverages of 5 Å. Only one broadened component is required to fit the 10 Å spectrum, which has comparable contributions from closely overlapping bulk and reacted components.

emission intensity to remain larger than that for Ga 3*d*. The latter incorporates both the metallic Ga and the bulk contributions, which is represented by the solid line. If the remnant P 2*p* component were solely of bulk origin, its attenuation curve would follow closely the solid line of the Ga 3*d* bulk component. Since this is not observed, we conclude that the principal contribution to the P 2*p* spectrum for coverages beyond 5 Å, where the Ga 3*d* and P 2*p* curves diverge in Fig. 8, is from a reaction product whose binding energy essentially equals that of the P 2*p* bulk component. Furthermore, this reaction product tends to diffuse to the top of the Cu layer, where it remains only slightly attenuated by additional Cu. The binding energy of this product suggests that it is not elemental P, which would be expected to lie, as for As on GaAs,[4] at a lower KE relative to the bulk component. The tendency of Cu-P compound formation and their phase diagram[34] suggests that the P is bonded to Cu in a definite stoichiometric but unknown ratio, a view supported by the constancy of its binding energy throughout the coverage range (to 30 Å). As an aside, the close overlap of the bulk and reacted components can lead to considerable uncertainties in the band-bending values for measurements that rely solely on the P 2*p* spectra. This point will be clarified in the next section, where we determine from the band-bending studies that the bulk and reacted components are separated by $<0.1$ eV.

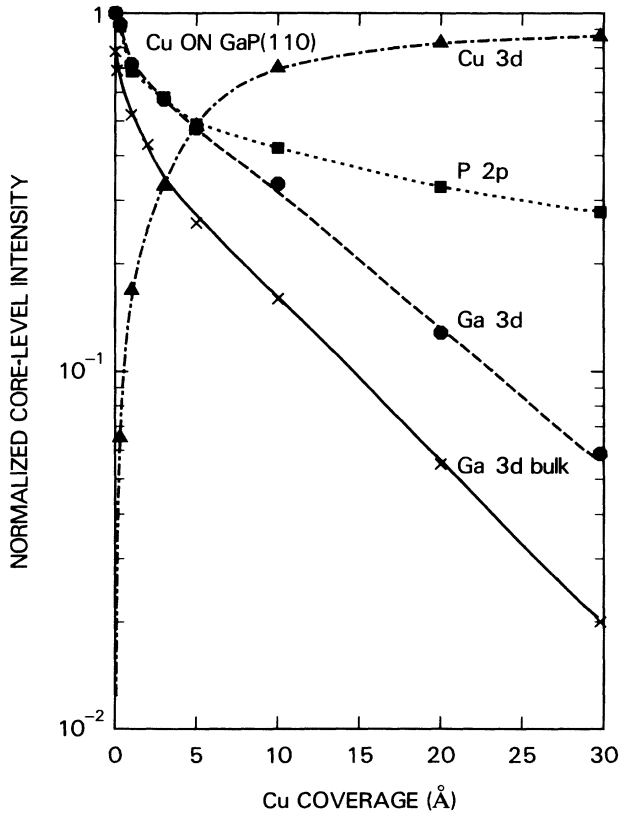


FIG. 8. Emission intensities of the P 2*p*, Ga 3*d*, and Cu 3*d* core levels as a function of Cu coverage. The solid curve is the bulk contribution to the Ga 3*d* signal calculated from the spectral decompositions of Fig. 6.

The evolution of the valence-band spectrum with Cu coverage is shown in Fig. 9. Again we show superimposed spectra for clean *n*-type GaP(110) [solid line, curve (a)] and for a Cu coverage of 0.01 Å ($\sim$0.01 ML, dotted curve), together with their difference [curve (b)]. The apparent lower sensitivity for Cu 3*d*, compared to Ag 4*d*, is largely due to the overlap of the Cu 3*d* emission with the

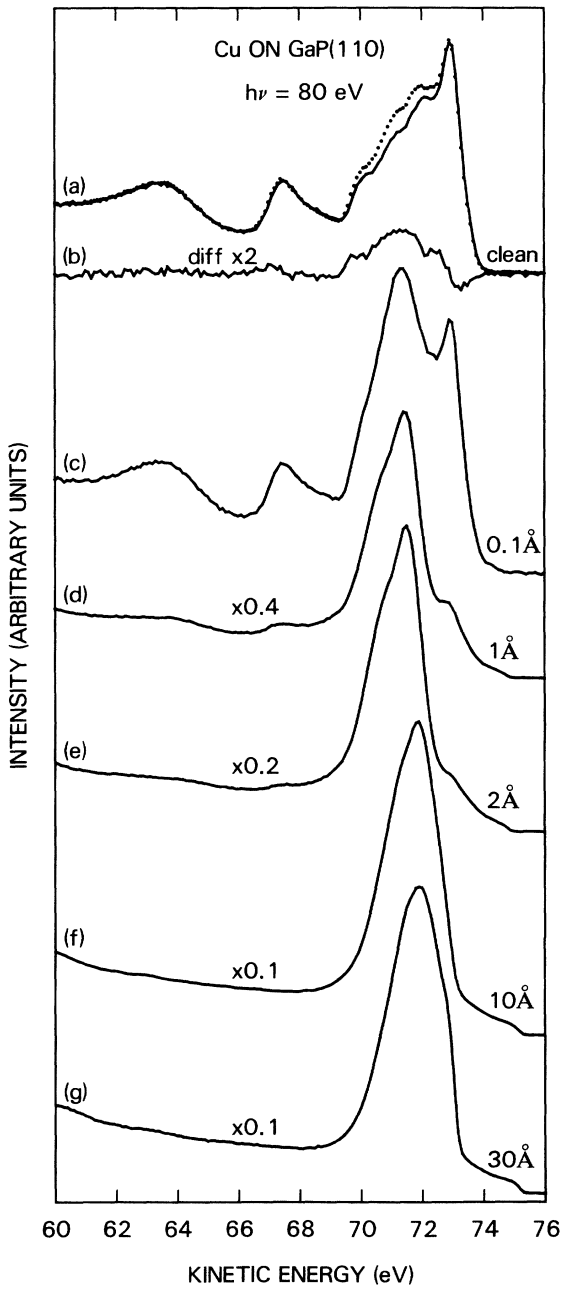


FIG. 9. Valence-band EDC's for clean and Cu covered GaP(110) surfaces. A spectrum for 0.01 Å Cu coverage (dotted curve) is superimposed on the clean spectrum (solid line) in curve (a). The magnified difference is shown in curve (b); its sole structure, due to Cu 3*d* emission, intensifies, and dominates the spectra at higher coverages [curves (c)–(g)], but does not broaden appreciably.

main valence-band structure of the GaP. As the coverage increases the Cu $3d$ contribution emerges from the background [curve (c)], and like Ag $4d$, totally dominates the valence-band spectrum for Cu coverages near 1 Å and beyond. A bulk Cu-like valence-band spectrum is only observed near 30 Å [curve (g)]. A possible reason for the larger thickness required for Cu to exhibit bulk-like spectral properties, compared to Ag, can be attributed to the additional presence of Ga and P reaction products in the thin Cu overlayers. The similarities of the spectra in the 1–10-Å range would suggest that the Cu overlayer displays metallic properties. However, the appearance of a Fermi edge is only obvious for Cu coverages beyond 2 Å, as shown in Fig. 10. As for Ag, emission due to filled states of largely Cu $4s$ origin extends into the gap region of the GaP before the appearance of the Fermi edge, as can be readily observed in spectrum (a) for 1 Å coverage. For such small coverages the Cu film is not continuous, but consists of clusters of Cu and Ga which are dispersed over the surface with regions of bare GaP exposed up to thicknesses of at least ~5 Å. A noticeable difference between Ag and Cu on GaP(110) is that the latter exhibits metallicity at thicknesses at least twice those for Ag, which suggests a lower surface mobility of the Cu atoms, an observation that is consistent with the greater reactivity of Cu.

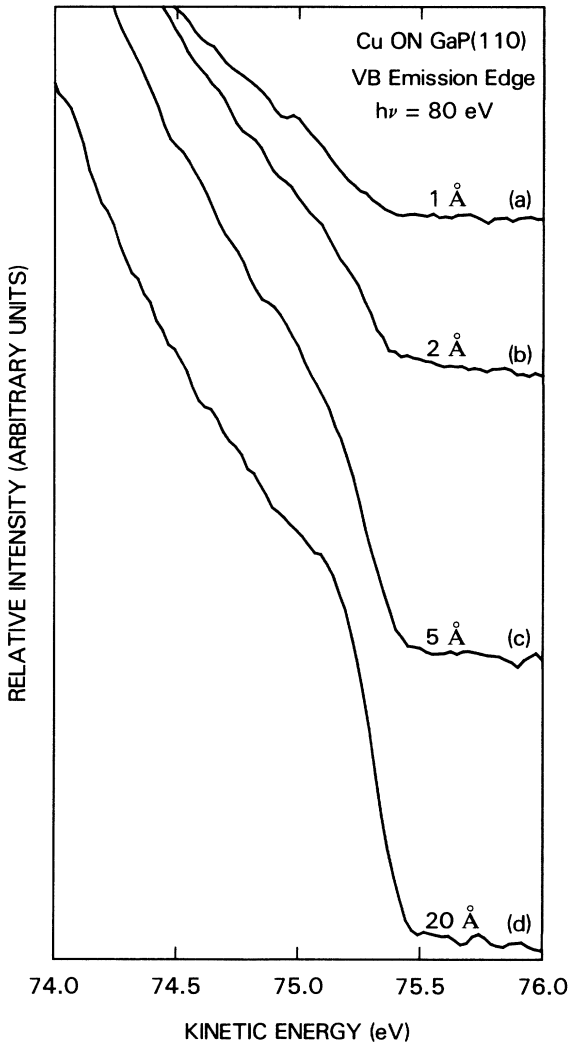


FIG. 10. Expanded view of the emission edge region of the valence-band EDC's for Cu on GaP(110). The appearance of a metallic Fermi edge is barely evident for a Cu coverage of 2 Å, curve (b).

### C. Au/AgP(110)

The effect of Au depositions on the Ga $3d$ core-level EDC's is shown in Fig. 11. The spectrum of the clean

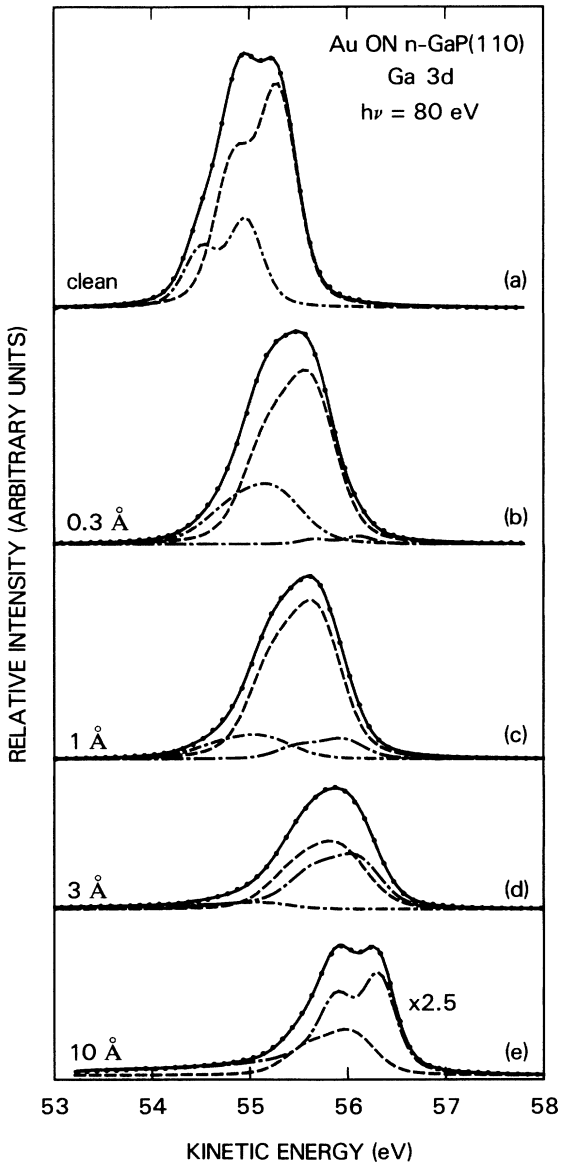


FIG. 11. Ga $3d$ spectra for indicated coverages of Au on $n$-type GaP(110). Component designations are the same as for Figs. 1 and 6.

surface, curve (a), again shows the detailed features of a good cleave, which are readily decomposed into bulk (dashed) and surface (dotted-dashed) contributions. Unlike Ag and Cu, the spectral features are rapidly broadened with moderate coverages of Au, e.g., for 0.3 Å depicted in curve (b), which suggests inhomogeneous band bending resulting from strong chemical interactions. Evidence for these can also be observed at this coverage by the weak structure on the high-KE side of the bulk line, and its rapid growth for larger Au coverages. Its energetic position relative to the bulk peak of ~0.3 eV remains unchanged with coverage and suggests that unlike the Cu case, the Ga never aggregates into metallic Ga [relative energy 0.72 eV (Ref. 31)], but rather remains dispersed in the Au, possibly in a unique bonding environment as previously proposed by Trafas *et al.*[26] The interaction of Au and GaP is substantially more intense than for Cu, as can easily be ascertained by comparing the spectra for the 10-Å depositions in Figs. 6 and 11. Some clustering of the Au appears to take place, as the surface component remains observable to coverages of 3 Å (~2 ML).

The P 2*p* spectra for corresponding Au coverages are shown in Fig. 12. Evidence for a reaction product is also observed for a Au coverage of 0.3 Å [curve (b)] on the low-KE side of the bulk peak. It continues to increase with coverage and remains at 0.68 eV below the bulk component. This value is somewhat larger than the value of 0.55 eV reported by Trafas *et al.*,[26] which was deduced from less resolved spectra. At first glance the bulk peak appears to remain dominant even at 10 Å [curve (e)]; but a comparison with the expected bulk intensity contribution in the Ga 3*d* spectrum [Fig. 11(e)] indicates that this apparent P 2*p* bulk peak must contain additional contributions from another reaction product. This conclusion is also supported by the attenuation curve of the P 2*p* intensity with Au coverage, shown in Fig. 13, which indicated that phosphorus (as well as Ga) remains in the vicinity of the surface. A similar conclusion was reached by Trafas *et al.*,[26] who also identified the reacted product

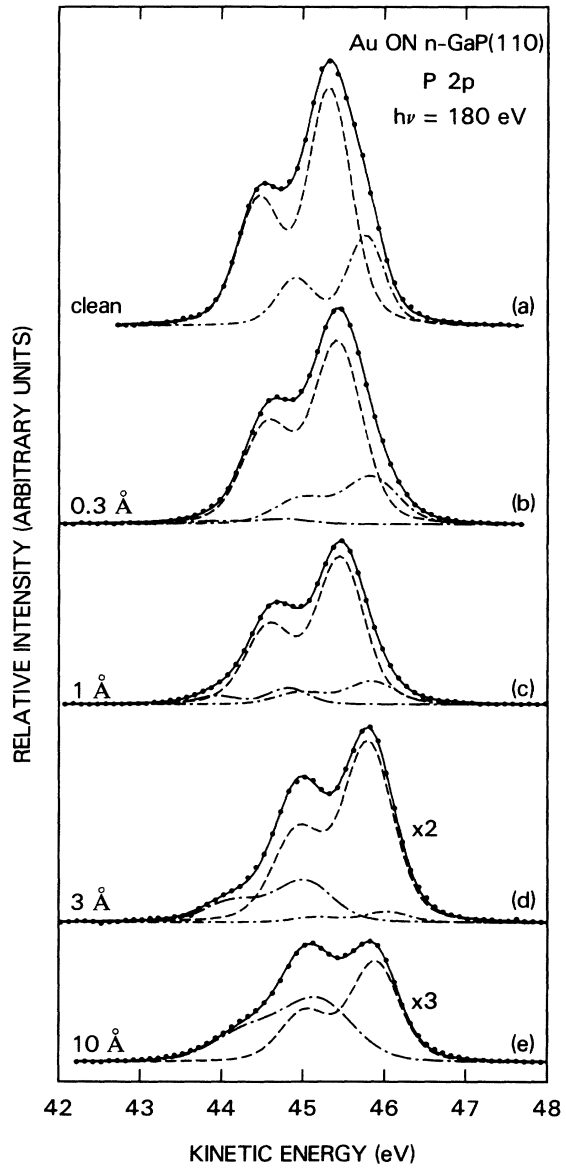


FIG. 12. P 2*p* spectra for indicated coverages of Au on *n*-type GaP(110). A reaction component, long dotted-dashed line, is already apparent for 0.3 Å coverage, curve (b), on the low-KE side of the dashed bulk component. The latter for 10 Å coverage, curve (e), includes, as for Cu, the bulk component and a large but unseparable reacted component.

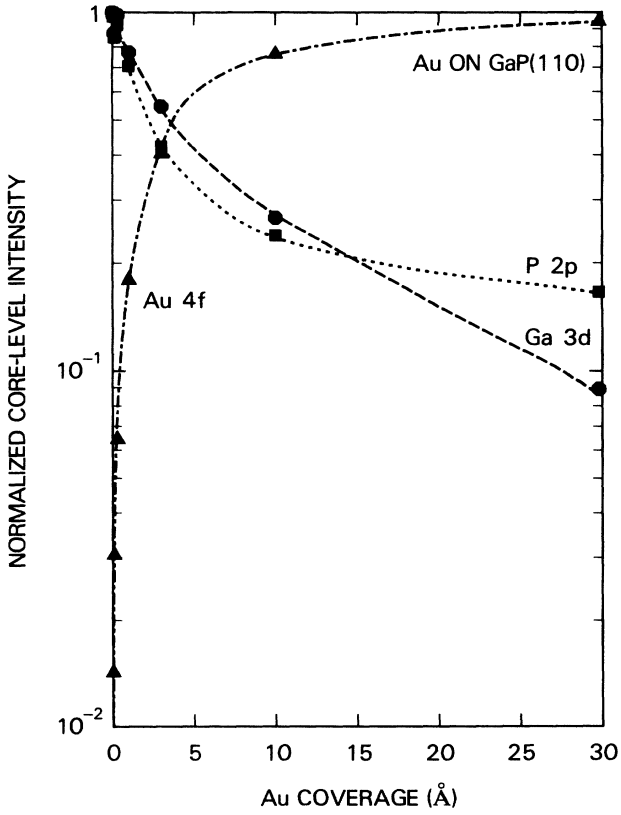


FIG. 13. Emission intensities of the P 2*p*, Ga 3*d*, and Au 4*f* core levels as a function of Au coverage.

as being distinct and separated by −0.38 eV from the bulk peak. From our Ga 3*d* data and the band-bending studies to be presented in the next section, we conclude that the binding energy of this P 2*p* component is well within 100 meV of that of the bulk peak; consequently, a separation of such overlapping spectra into two closely separated components is quite arbitrary, unless constraint by complementary data from the Ga 3*d* spectra. This coincidence of the two P 2*p* peaks is similar to the Cu case, which would suggest that similar chemical environment may apply for the two cases. Trafas *et al.*[26] suggested elemental P as the origin for this component for Au, whereas they assign the lower-lying reacted component to P dispersed in Au. For Cu we argued that the reacted component implies P—Cu bonding; a similar situation is not obvious for Au, as at most a single metastable Au-P compound has been reported and the solubility of P in Au appears to be low.[34] However, we do not concur with its previous assignment to elemental P, which, as for As/GaAs, should lie on the high-binding-energy (low-KE) side of the bulk peak. Consequently, we will tentatively assign the low-KE reacted component to elemental P, and the higher-lying one to P weakly bonded to Au, with both components segregating to the surface. Also shown in Fig. 13 is the intensity of the Au 4*f* emission normalized to the thick-coverage intensity. Its rapid initial rise for submonolayer coverages (<2 Å) is sublinear even for a linear plot, which is indicative of clustered growth. This tendency is also manifested in Fig. 13 at higher coverages, at which the Au 4*f* curve increases substantially slower than expected for nonclustered growth. Thus the strong tendency for three-dimensional growth for Au on GaP(110) is analogous to observations of Au on GaAs(110).[35]

The tendency for clustering is also apparent in the valence-band spectra, shown in Fig. 14. Curve (a) is a composite of a spectrum of the clean surface (solid line) and that for a coverage of ~0.003 Å (0.002 ML, dotted curve). Their difference, shown in curve (b), consists of a single, albeit somewhat noisy peak, whose origin derives from the Au 5*d* states, as can be readily ascertained from the spectra at higher coverages. This single peak suggests that for our lowest coverages the Au consists predominantly of single atoms dispersed over the surface. A spectrum for a coverage of 0.03 Å is shown in curve (c). Its difference spectrum with that for the clean surface is shown in curve (d), which already exhibits a splitting of the Au 5*d* structure that is indicative of aggregation of the Au atoms. This splitting increases with coverage as the Au clusters and eventually assumes full metallic characteristics. Only minor changes in line shape are observed for Au coverages beyond 10 Å. Full metallic characteristics are not observed until 3 Å of Au have been deposited, which can be inferred from the appearance of a Fermi edge, as shown magnified in the inset. Emission at the Fermi edge becomes more obvious for higher coverages, as shown, for example in curve (g) for 10 Å. Thus, compared to Ag and Cu, the formation of the Au Fermi edge requires the largest deposit of the metal. This observation appears to be related to the degree of reactivity, which reduces the surface mobility (smaller clusters) and enhances intermixing of the metal and reaction products, features that are likely to delay the onset of metallicity.

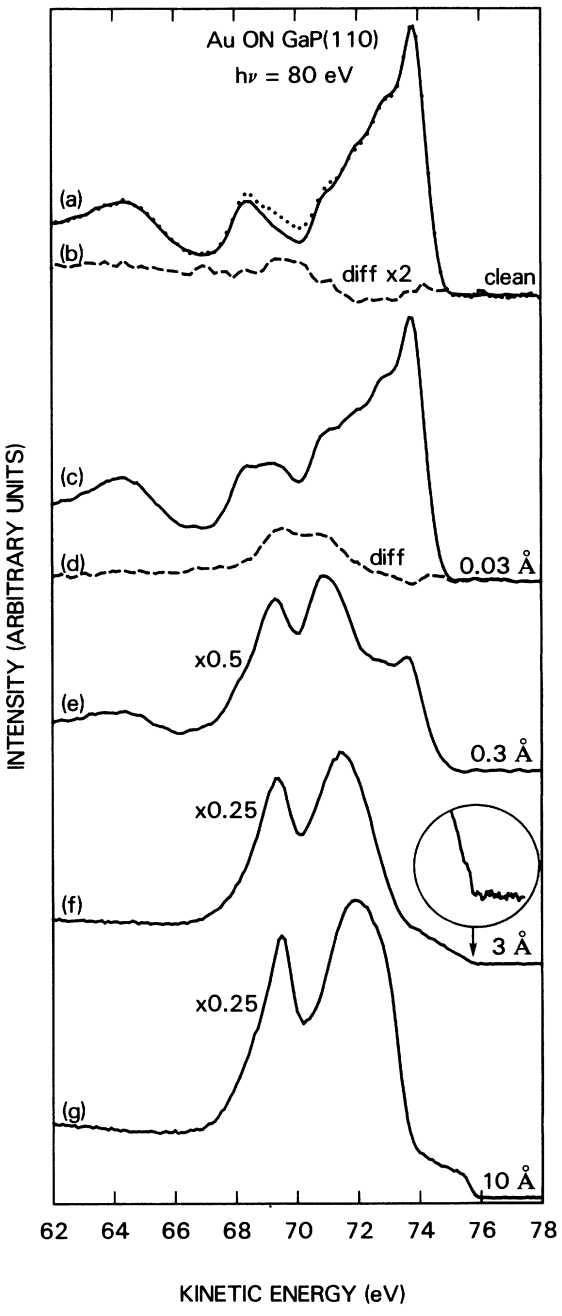


FIG. 14. Valence-band EDC's for Au on GaP(110). Superimposed on the clean-surface spectrum [solid line, curve (a)] is the dotted curve for 0.003 Å coverage. Their difference, curve (b), shows a single emission structure due to Au 5*d* electrons. Curves (c) and (d) correspond, respectively, to 0.03 Å coverage and its difference spectrum with the clean surface. The Au 5*d* splitting increase with coverage, curves (e)–(g). A metallic Fermi edge is only observable at coverages $\gtrsim 3$ Å of Au, as shown in the inset for curve (f).

## IV. BAND-BENDING STUDIES

The changes in the position of the Fermi level relative to the VBM for $n$- and $p$-type GaP(110), deduced from the bulk components of the Ga $3d$ and P $2p$ emission spectra, are shown in Figs. 15(a)–(c) as a function of coverage of the three metals. The amount of band bending is determined by the separation of $E_F$ from the conduction-band minimum (CBM) at 2.26 eV for $n$-type substrates, and from the VBM for $p$-type substrates. Unlike GaAs(110), for which flat-band conditions are readily achieved for $p$-type samples, cleaved GaP(110) generally exhibits appreciable band banding on both $n$- and $p$-type substrates. Consequently, the determination of the position of $E_F$ for the cleaved surface becomes somewhat problematic, as one must determine the top of the valence band from its spectrum. The technique generally used is simply to consider a straight-line approximation to the valence-band emission edge and declare its intersection with the zero-emission background as the VBM. The validity of this approach is supported by a detailed analysis of the valence-band structure.[36] For lack of a better method, we take the same approach here. There are some caveats about this approach for surfaces that are already exhibiting band bending, as for most GaP(110) surfaces.[25,26,29,30] This phenomenon, being generally inhomogeneous for a freshly cleaved surface, introduces structure in the valence-band edge, including tails, which render the aforementioned method for the VBM determination somewhat arbitrary. By using both $n$- and $p$-type substrates, this uncertainty is greatly reduced by cross referencing the deduced VBM for the clean surfaces with the energetic separation of their core levels. The results shown in Fig. 15 were obtained by this approach. Because of the difficulties of separating bulk and reacted components in the P $2p$ spectra for Cu and Au above $\sim 5$ Å, we disregard the high-coverage P $2p$ data in the determination of the band bending. The lines drawn through the points represent the best fit to the most reliable data. Uncertainties in the absolute position (relative to the VBM) of $E_F$ is less than $\pm 0.1$ eV for the three metals, whereas the uncertainty of the relative differences of $E_F$ among the three metals is less than $\pm 0.05$ eV.

The curves for Ag and Cu on $n$-type GaP are characterized by a nearly constant value of $E_F$ over much of the sub-angstrom coverage region. This suggests that the Ag and Cu atoms induce nearly-coverage-independent acceptor levels, labeled $E_1^0$ in Fig. 15, which are independent as well of the initial band bending and differ, as stated in the last section, from the cleavage-induced levels. Au exhibits a narrower region of constant or nearly constant $E_F$ below 1 Å, indicating that its acceptor level varies with coverage, a consequence, perhaps, of the more reactive nature of the Au/GaP interface. On $p$-type substrates all three metals produce a similar behavior in the coverage dependence of the Fermi level, which consists of an initial increase in $E_F$, followed by a plateau near 0.5 Å and a subsequent decrease at higher coverages. This effect is referred to as an overshoot. Coinciding with the appearance of metallic characteristics in the overlayer, as determined from the appearance of an Fermi edge, $E_F$ drops in the band gap for all three metals on both $n$- and $p$-type substrates. Of equal significance is the observation that, following this drop, the positions of $E_F$ on $n$- and $p$-type GaP coincide. Both observations are the consequence of the dominance of metallic states in the determination of the ultimate position of $E_F$, and are in general agreement with results obtained for metal/GaAs(110) interfaces formed at room temperature.[4–6,8,17,33]

## V. DISCUSSION

Table I summarizes prior determinations of Schottky-barrier heights for the three metals on GaP. Most data represent electrical measurements on devices prepared under diverse conditions, with the exception of the photoemission (PE) results of Brillson *et al.*[25] and this work on similarly prepared surfaces. Consequently, we will discuss these results first. There is some disagreement in the absolute values of the barrier heights for Au and Ag in these measurements. These discrepancies may arise both from a lower spectral definition (resolution) in the reported spectra of Brillson *et al.*[25] and in their omission to extract rigorously the bulk components from their spectra. Our own values, whose absolute accuracy is better than $\pm 0.1$ eV, lie on the higher end of barrier heights for all three metals, with Au lying slightly outside

TABLE I. Summary of previous and present determinations of Schottky-barrier heights, in eV, for Au, Ag, and Cu on $n$-type GaP. The last row corresponds to barrier heights determined by use of the delocalization model (Ref. 16).

| Surface orientation | Au | Ag | Cu | Method | Reference |
|---|---|---|---|---|---|
| not given | 1.52 | 1.44 | 1.44 | *I-V* | 38 |
| (111) | | | 1.26 | *I-V* | 24 |
| (111) | | | 1.30 | *C-V* | 24 |
| not given | 1.30 | 1.14 | 1.31 | *I-V*, *C-V* | 23 |
| (111) | 1.42 | 1.38 | | *I-V* | 39 |
| $(\bar{1}\bar{1}\bar{1})$ | 1.52 | 1.51 | | *I-V* | 39 |
| (110) | 1.38 | | 1.25 | PE | 25 |
| (110) | 1.55 | 1.37 | 1.41 | PE | this work |
| any | 1.65 | 1.32 | 1.39 | deloc. model | this work |

the range of values determined by the electrical measurements. However, the latter values exhibit considerable scatter, which makes them unsuitable as reference values. Since the difference of our measured values of the Schottky barriers for Ag and Au is only 0.18 eV, compared to a work-function difference of ~0.8 eV,[37] our results imply strong deviations from ideal Schottky-Mott behavior. This observation is consistent with prior electrical measurements,[23,24] but disagrees with the prior photoemission results.[25] However, systematic photoemission studies on both $n$- and $p$-type GaP over a broader metal work-function range are needed before a final assessment can be made on the claimed ideality of the metal-GaP(110) system.[25] For comparison, we also show in Table I values for Schottky-barrier heights derived from the delocalization model,[16] which is based on the properties of the pure metal, and thus does not include the influence of alloying on the interface properties.

The delocalization model assumes the existence of a large interface density of states whose origin derives from acceptorlike defect or impurity states that are generated during the metal-deposition process. These states are discrete prior to the onset of metallicity in the overlayer and are the states responsible for determining the Fermi level for the submonolayer coverages of the noble metals on $n$-type GaP(110) shown in Fig. 15. We assume the nearly constant $E_F$ to lie in close proximity to the adsorbate-induced acceptor levels, which are labeled $E_i^0$ in Fig. 15. The presence of the developing metallic overlayer broadens these levels into resonances through the interaction of the metallic and impurity wave functions.[16] The resonances assume the role of an interface density of states which can accept the charge required for the establishment of an interface dipole that equalizes the Fermi level on both sides of the junction. The degree of charging is proportional to the difference between the ionization energy of the semiconductor, $I_{sc}$ and the metallic work function $\phi_m$, and is therefore small for the larger-work-function metals. The small interface charge for such metals implies that the Fermi level lies low in the resonances and hence produces a large Schottky-barrier height on $n$-type substrates.[16] The formalism of the model is particularly suited to calculate the changes in the Fermi level ($\Delta E_F$) during the metallization process, as the defect level $E_i^0$ is known from the experimental data. Under equilibrium conditions the Fermi level is given by

$$E_F=(I_{sc}-\phi_m)-4\pi\lambda_{eff}e^2N_i q_{eff} . \quad (1)$$

The last term in Eq. (1) is the interface-dipole contribution, whose factors represent the density of impurity states at the interface $N_i$ ($\sim 5\times10^{14}$ cm$^{-2}$), the dipole charge separation $\lambda_i$ ($\sim 1$ Å), and the effective charge per resonance $q_{eff}$. The latter charge, which is generally less than $0.1|e|$, is obtained from self-consistent solutions of Eqs. (1) and (2) of Ref. 16, with a Lorentzian broadening parameter $\Gamma=0.11$ eV.[16] The change in $E_F$ is simply given by

$$\Delta E_F=E_F-E_i^0 . \quad (2)$$

For $I_{sc}=6.01$ eV,[29] and $\phi_m$'s for polycrystalline metals[37] in Eq. (1), we obtain the following values for $\Delta E_F$: $-0.21$ ($-0.27$), $-0.40$ ($-0.44$), and $-0.54$ ($-0.50$) eV for Ag, Cu, and Au, respectively, which compare favorably with the experimental values given in parentheses. As for GaAs,[17] we may calculate Schottky-barrier heights based on a "universal" defect level, which for simplicity we assume to lie at mid gap (1.13 eV). Using the same procedure as before, we obtain the Schottky-barrier heights $\Phi_B^n$ ($=1.13-\Delta E_F$) for the noble metals on $n$-type GaP(110) listed in Table I.

The generally good agreement of the predictions of the delocalization model, both in the changes of $E_F$ with metallization, and the magnitudes of Schottky-barrier heights, supports, as for GaAs, the basic premises of the model. These include the dominant role of defect or impurity states in determining $E_F$ for metal coverages near a monolayer, and the strongly perturbing influence of the metallic states on the impurity levels once the overlayer becomes metallic. The model thus has great similarities

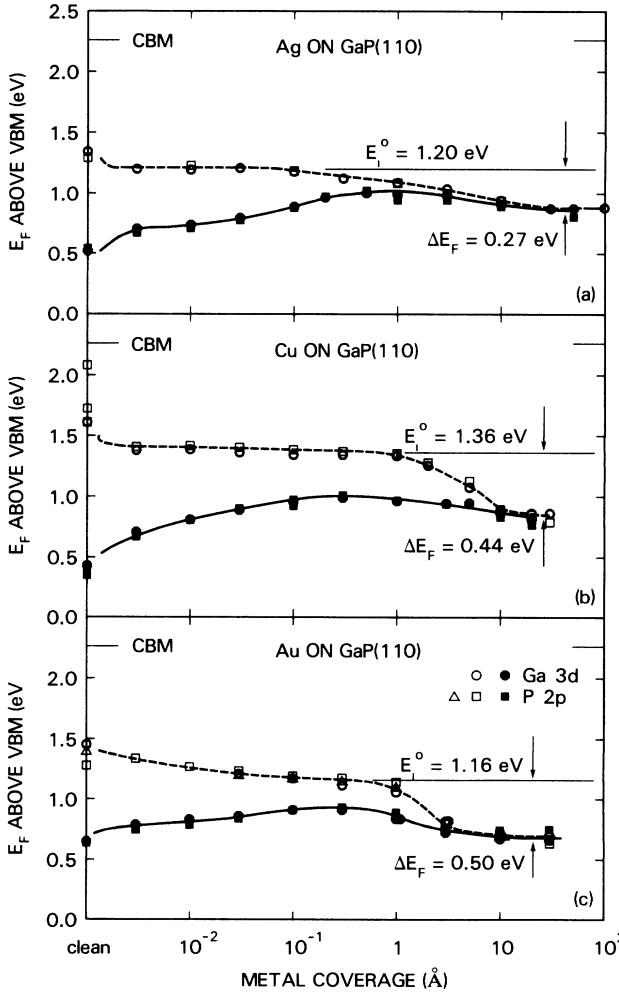


FIG. 15. The evolution of the interfacial Fermi level $E_F$ with metal coverage on $n$- and $p$-type GaP(110) for (a) Ag, (b) Cu, and (c) Au. $E_i^0$ marks the energy of a metal-adatom–induced acceptor level. $\Delta E_F$ is the change in $E_F$ due to the development of metallic characteristics in the overlayer.

with the metal-induced gap-state models,[11–15] but unlike these the delocalization model includes the presence of defect states and their modifications (delocalization) in the presence of metallic states. The delocalization model includes an intrinsic variation of barrier heights with metallic work functions, which the MIGS models generally lack.[14,15] The latter shortcoming is also inherent to the universal defect model of the Schottky barrier,[2] which also cannot account for the observed large variations in $E_F$ with onset of metallicity.

It is relevant at this stage to comment on the possible effects of photon-induced band-bending changes (photovoltage effects) during the photoemission experiments. This effect has been invoked recently[40] to explain the coverage-dependent evolution of the Fermi-level position on GaAs near 100 K measured by photoemission spectroscopy excited with synchrotron radiation.[9,10] These results are characterized by a nearly-coverage-independent position of $E_F$ high in the band gap on $n$-type GaAs, followed by a rapid drop towards midgap for metal coverages exceeding $\sim 1$ Å. Furthermore, the positions of $E_F$ on $n$- and $p$-type GaAs, unlike the room-temperature studies, remain separated up to the maximum metal coverages for which the core-level data could still be extracted ($\sim 10$ Å). Although dominant at low temperatures, photovoltage effects could still be influential at room temperature for low-doped samples under extreme irradiation conditions. In fact, Alonso *et al.*[41] recently attributed the "delayed" convergence of the $E_F$'s at room temperature for silver on $n$- and $p$-type GaP(110) to photovoltage effects produced by the high-intensity synchrotron radiation of their undulator beamline. They also observed coverage-dependent Fermi-edge energies for Ag, which they attributed to the same effect, and used these values to correct their band-bending data. The corrected curves are in good agreement with our results of Fig. 15(a). Based on this agreement, as well as the lack in energy shifts of the metallic Fermi edges for our metal overlayers and the convergences of $E_F$ for all three noble metals on $n$- and $p$-type GaP, we conclude that under our experimental conditions photovoltage effects play a minor role ($< 0.05$ eV).

We would like to comment briefly on the question of the existence of intrinsic gap states derived from the Ga dangling bonds. The assumption of their presence, $\sim 1.7$ eV above the VBM, was based on the observation of contact-potential differences consistently less than the expected band-gap value.[29] Subsequent failures by various workers to achieve flat-band cleaves for $n$-type GaP(110) appeared to support this view. However, recently Chiaradia *et al.*[30] reported the achievement of a limited number of cleaves that indicated near-flat-band conditions. The position of $E_F$ was deduced from estimates of the VBM in their valence-band EDC's. One of our $n$-type cleaves for the Cu depositions [Fig. 15(b)] suggested as well that we had achieved near-flat-band conditions ($E_F \sim 2.1$ eV above the VBM). This conclusion was supported by an unusually high energetic difference (1.73 eV) between the bulk Ga $3d$ component for this cleave and the corresponding component for a well-cleaved $p$-type surface in the same series. Both points are indicated in Fig. 15(b). $E_F$ on most of the $n$-type cleaves, however, fell in the range 1.4–1.7 eV, and thus exhibited initial band bending of 0.4–0.7 eV, comparable to the values observed on the $p$-type cleaves. The latter surfaces consistently exhibited emission structure of lower apparent resolution than those on $n$-type material. As stated earlier, the lower apparent resolution is generally attributed to band bending that is not homogeneous across the surface. The observation that the $n$-type emission structure is consistently sharper, with little difference between the flat-band cleave and those with considerable more band bending, suggests that the defect levels on $n$-type surfaces are energetically and spatially more homogeneous than their $p$-type counterparts, which would suggest that their origins are differently as well. The above observations are consistent with our previous arguments against the importance of photovoltage effects in the present studies, since the dominance of such effects would otherwise result in energy differences between the core levels of freshly cleaved $n$- and $p$-type GaP that are consistently near the band-gap value, as well as yield line shapes that are characteristic of flat-band conditions.

## ACKNOWLEDGMENTS

We would like to acknowledge the technical assistance of M. Prikas, A. Marx, D. Costas, and the staff of the National Synchrotron Light Source at Brookhaven National Laboratory (Upton, NY), a facility supported by the U.S. Department of Energy (Division of Materials Sciences and Division of Chemical Sciences of the Office of Basic Energy Sciences). We would also like to thank M. Prietsch for helpful discussions and comments on this paper.

*Present address: Department of Physics, Queen's University, Kingston, Ontario, Canada K7L 3N6.

†Present address: Laboratoire pour l'Utilisation du Rayonnement Electromagnétique (LURE), Université de Paris–Sud, Orsay 91405, France.

[1] E. H. Rhoderick and R. H. Williams, *Metal Semiconductor Contacts* (Clarendon, Oxford, 1988).

[2] W. E. Spicer, P. W. Chye, P. R. Skeath, C. Y. Su, and I. Lindau, J. Vac. Sci. Technol. **16**, 1422 (1979); W. E. Spicer, I. Lindau, P. R. Skeath, and C. Y. Su, *ibid.* **17**, 1019 (1980).

[3] L. J. Brillson, in *Handbook of Synchrotron Radiation*, edited by G. V. Marr (North-Holland, Amsterdam, 1985), Vol. II.

[4] R. Ludeke and G. Landgren, Phys. Rev. B **33**, 5526 (1986).

[5] M. Prietsch, M. Domke, C. Laubschat, and G. Kaindl, Phys. Rev. Lett. **60**, 436 (1988).

[6] K. Stiles and A. Kahn, Phys. Rev. Lett. **60**, 440 (1988); K. Stiles, S. F. Horng, A. Kahn, J. McKinley, D. G. Kilday, and G. Margaritondo, J. Vac. Sci. Technol. B **6**, 1392 (1988).

[7] G. Jezequel, A. Taleb-Ibrahimi, R. Ludeke, and F. Schäffler, J. Vac. Sci. Technol. A **6**, 1561 (1987).

[8]G. Hughes, R. Ludeke, F. Schäffler, and D. Rieger, J. Vac. Sci. Technol. B **4**, 924 (1986).
[9]K. Stiles, A. Kahn, D. G. Kilday, and G. Margaritondo, J. Vac. Sci. Technol. B **5**, 987 (1987).
[10]R. Cao, K. Miyano, T. Kandelewicz, K. K. Chin, I. Lindau, and W. E. Spicer, J. Vac. Sci. Technol. B **5**, 998 (1987).
[11]V. Heine, Phys. Rev. **138**, A1689 (1965).
[12]S. G. Louie, J. R. Chelikowsky, and M. L. Cohen, Phys. Rev. B **15**, 2154 (1977).
[13]E. J. Mele and J. D. Joannopoulos, Phys. Rev. B **17**, 1528 (1978).
[14]E. Louis, F. Yndurain, and F. Flores, Phys. Rev. B **13**, 4408 (1976).
[15]J. Tersoff, Phys. Rev. Lett. **52**, 465 (1984); Phys. Rev. B **32**, 6968 (1985).
[16]R. Ludeke, G. Jezequel, and A. Taleb-Ibrahimi, Phys. Rev. Lett. **61**, 601 (1988); J. Vac. Sci. Technol. B **6**, 1277 (1988); Appl. Surf. Sci. **41**, 151 (1989).
[17]R. Ludeke, Phys. Rev. B **40**, 1947 (1989); R. Ludeke, in *Metallization and Metal-Semiconductor Interfaces,* Vol. 195 of *NATO Advanced Study Institute, Series B: Physics,* edited by I. Batra (Plenum, New York, 1989), p. 39.
[18]N. Newman, M. van Schlifgaarde, T. Kendelewicz, M. D. Williams, and W. E. Spicer, Phys. Rev. B **33**, 1146 (1986).
[19]A. B. McLean and R. H. Williams, J. Phys. C **21**, 783 (1988).
[20]R. Ludeke, T. -C. Chiang, and T. Miller, J. Vac. Sci. Technol. B **1**, 581 (1983).
[21]W. Mönch, J. Vac. Sci. Technol. B **6**, 1270 (1988).
[22]I. Lindau, P. W. Chye, C. M. Garner, P. Pianetta, C. Y. Su, and W. E. Spicer, J. Vac. Sci. Technol. **15**, 1332 (1978).
[23]T. F. Lei, C. L. Lee, and C. Y. Chang, Solid-State Electron. **22**, 1035 (1979).
[24]T. A. Laperashvili and G. A. Nakashidze, Zh. Tekh. Fiz. **55**, 733 (1985) [Sov. Phys.—Tech. Phys. **30**, 433 (1985)].
[25]L. J. Brillson, R. E. Viturro, M. L. Slade, P. Chiaradia, D. Kilday, M. K. Kelly, and G. Margaritondo, Appl. Phys. Lett. **50**, 1379 (1987); P. Chiaradia, L. J. Brillson, M. Slade, R. E. Viturro, D. Kilday, N. Tache, M. Kelly, and G. Margaritondo, J. Vac. Sci. Technol. B **5**, 1075 (1987).
[26]B. M. Trafas, F. Xu, M. Vos., C. M. Aldao, and J. H. Weaver, Phys. Rev. B **40**, 4022 (1989).
[27]A. B. McLean and R. Ludeke, Phys. Rev. B **39**, 6223 (1989).
[28]S. Doniach and M. Šunjić, J. Phys. C **3**, 285 (1970).
[29]J. van Laar, A. Huijser, and T. L. van Rooy, J. Vac. Sci. Technol. **14**, 894 (1977).
[30]P. Chiaradia, M. Fanfani, P. Nataletti, P. De Padova, L. J. Brillson, M. L. Slade, R. E. Viturro, D. Kilday, and G. Margaritondo, Phys. Rev. B **39**, 5128 (1989).
[31]A. Taleb-Ibrahimi, G. Jezequel, and R. Ludeke, J. Vac. Sci. Technol. B **6**, 1427 (1988).
[32]J. J. Yeh and I. Lindau, At. Data Nucl. Data Tables **32**, 1 (1985).
[33]K. Stiles, A. Kahn, D. Kilday, and G. Margaritondo, J. Vac. Sci. Technol. A **6**, 1511 (1988).
[34]*Binary Alloy Phase Diagrams,* edited by T. B. Massalski (American Society for Metals, Metals Park, OH, 1986), Vol. I.
[35]R. M. Feenstra, Phys. Rev. Lett. **63**, 1412 (1989); J. Vac. Sci. Technol. B **7**, 925 (1989).
[36]E. A. Kraut, R. W. Grant, J. R. Waldrop, and S. P. Kowalczyk, Phys. Rev. Lett. **44**, 1620 (1980).
[37]*Handbook of Chemistry and Physics,* 70th ed., edited by R. C. Weast (Chemical Rubber Co., Boca Raton, FL, 1989), p. E93.
[38]N. T. Tam and Tran Chot, Phys. Status Solidi A **93**, K91 (1986).
[39]M. Kusaka, N. Hiraoka, M. Hirai, and S. Okazaki, Surf. Sci. **91**, 264 (1980); measurements for *p*-type GaP, converted by subtracting values from the GaP band gap of 2.26 eV.
[40]M. H. Hecht, J. Vac. Sci. Technol. (to be published).
[41]M. Alonso, R. Cimino, Ch. Maierhofer, and K. Horn, J. Vac. Sci. Technol. B (to be published); M. Alonso, R. Cimino, and K. Horn, Phys. Rev. Lett. **64**, 1947 (1990).